

Heat Transfer and Wall Temperature Distribution during Flow Boiling In Conventional and Mini Channels

Arvind Kumar¹, Hardik Kothadia^{1*}

¹Mechanical Engineering Department
Indian Institute of Technology, Jodhpur
India, 342030
kumar.142@iitj.ac.in; hardikkothadia@iitj.ac.in*

Abstract - The fluctuation of pressure in flow boiling is affected due to liquid-vapor phase interaction, and thus the flow and wall temperature are influenced. The temporal and spatial variation of wall temperature and the heat transfer coefficient are investigated experimentally at atmospheric system pressure. The two mini-tubes of 2×300 and 4×600 mm inner diameter× heated length are used for analysis. The thermal image technology is used to show the wall temperature distribution. The experimental setup is validated by comparing the heat transfer coefficient with Dittus-Boelter and Gnielinski correlations. The boiling heat transfer coefficient in both tubes are compared to get the effect of diameter, mass flux and heat flux. The radially as well as axially variation of wall temperature during flow boiling is represented. The wall temperature during liquid-phase flow is identical in the radial direction and increases linearly in the axial direction. The wall temperature exhibits significant axially as well as radially variation in two-phase flow. The wall temperature fluctuates vigorously in mini-channels. The influence of subatmospheric system pressure on subcooled flow boiling is examined in the conventional channel with a diameter of 11.7 mm. An increase in the subcooled flow boiling heat transfer coefficient is observed when the system pressure is lower than atmospheric pressure. At subatmospheric system pressure, the wall temperature exhibits radial symmetry across all Froude number values. Furthermore, the mass flux does not significantly impact the subcooled boiling heat transfer coefficient, when subjected to constant heat flux.

Keywords: Flow boiling, temperature distribution, heat transfer coefficient, mini-channel, circular tube

1. Introduction

Flow boiling is used significantly in petrochemical, power plants, chemical plants, steam generators, high-temperature recuperators, synthetic natural gas industries, stator cooling, nuclear plants, and process industries [1]. Flow boiling is preferred due to its advantage of massive heat transfer of the sensible and latent heat compared to single phase heat transfer. The flow boiling in the circular tubes has been researched broadly to get heat transfer coefficient and pressure drop for many decades. As the miniaturization of mechanical devices is of prime interest, the smaller diameter tubes need to be researched. The smaller diameter tubes are used in refrigeration industries with the development of small tonnage units.

Deployment of two-phase technology necessitates an inclusive understanding of thermal characteristics of phase transformation in various channels. The capability to precisely forecast the flow boiling heat transfer for a specific channel geometry and operating conditions is of supreme importance to performance valuation and the design of mini-channel systems. Significant research has been conducted to get the heat transfer mechanism during flow boiling in mini-channels of different geometries at different operating parameters using different working fluids.

Kandlikar [2] performed experiments using water in a rectangular channel of 1×1×60 mm at 80 – 560 kg/m²s mass flux to get the flow oscillations using high-speed photography. They observed large pressure fluctuations attributed to the flow boiling phenomenon. Flow oscillations linked to pressure fluctuations often leads to flow reversal.

Kasza [3] performed experiments using water for bubbly and slug flow regime in a rectangular channel of 2.5×6×500 mm at a mass flux of 21 kg/m²s and 110 kW/m² heat flux. They found that the increased bubbles on the nucleation sites on the wall having a thin layer of liquid increase the heat transfer in small channels.

Yu [4] used a tube of 2.98 mm diameter and 910 mm length using water at 50 – 200 kg/m²s mass flux. They concluded that the boiling heat transfer of water in small channels depends on heat flux but majorly on mass flux. The nucleate boiling dominates over convective boiling in small channels up to vapor quality 0.5.

Flow boiling is influenced by inertia force, buoyancy force, and surface tension force, which impact the vapor generation rate, size, and frequency [5]. However, subatmospheric system pressure alters the behavior of these forces due to changes in the working fluid's characteristics. The latent heat of vaporization increases at subatmospheric system pressure, while the saturation temperature decreases, making it suitable for applications with restrictions on higher surface temperatures, such as electronic equipment cooling. The investigation of heat transfer at subatmospheric system pressure holds significance for various applications, including aircraft at high-altitude locations [6], future crewed habitats on the lunar surface [7], water desalination [8], heat pipes [9], etc. Many industries, such as food drying, rapid cooling, the medical sector, ocean thermal energy conversion (OTEC), and paper sheet drying, utilize subatmospheric system pressure [10].

The heat transfer coefficient in flow boiling is influenced by thermodynamic mass quality, heat flux, mass flow rate, geometry, orientation, and working fluid properties. The vapor quality and thermophysical characteristics of the flowing fluids are functions of the operating pressure. As a result, the phenomena and governing forces required for flow boiling change with system pressure and geometrical scale. Hence, investigating flow boiling in straight tubes is essential at subatmospheric system pressures.

In their experimental study, Colgan et al. [7] examined the nucleation characteristics at the subatmospheric system pressures using distilled water in a vertically oriented square channel having 12.7 mm hydraulic diameter. The research focused on the bubble diameter and frequency of departing bubbles under subatmospheric system pressure conditions. Their findings revealed that the diameter of departing bubbles increases at lower system pressures, while frequency of bubble departures is reduced.

In their work, Colgan et al. [11] established a relationship for critical heat flux (CHF) under subatmospheric system pressure conditions using a vertically oriented square channel. Their study identified the density ratio, Weber number, and Boiling number as the primary factors governing the correlation. Furthermore, they found that as the working pressure rises, the CHF value also rises. However, the effects of mass flux and inlet subcooling on CHF were observed to be relatively minor.

In their study, Latsch et al. [12] investigated nucleation under subatmospheric system pressure conditions using water in a vertically oriented tube with a diameter of 12 mm. The authors found that the air absorption characteristics of water are reduced at subatmospheric pressure. As a result, the non-condensable presence does not significantly impact the heat transfer coefficient under these conditions. Additionally, the higher vapor volume encountered at subatmospheric system pressure leads to increased flow instabilities.

In their investigation, Chang et al. [13] studied subcooled flow boiling on a micro silicon chip using FC-72 to examine bubble characteristics and heat transfer. Their findings indicated that increasing the inlet subcooling led to a decrease in the heat transfer coefficient, while the mass flux has a relatively minor impact on heat transfer coefficient. Furthermore, increasing the inlet subcooling and mass flux resulted in reduced bubble diameters and nucleation site density. On the other hand, an increase in heat flux led to larger bubble diameters, higher departure frequency of bubbles, and increased density of nucleation sites.

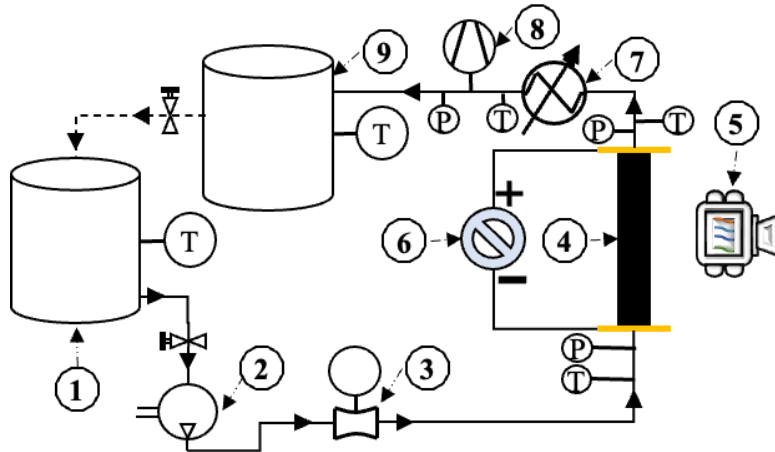
The existing literature on subcooled boiling mainly focuses on bubble diameter and frequency under subatmospheric system pressure, particularly in pool boiling or micro-channels. However, there is a lack of experimental data on heat transfer coefficient during subcooled boiling using water in straight tubes under subatmospheric system pressure conditions. To bridge this research gap, our study focuses on conducting experiments at absolute system pressures of 50, 75, and 101 kPa, with particular emphasis on the conventional channel. The classification of conventional and mini-channels is determined based on hydraulic diameters similar to those proposed by Kandlikar for both types of channels. The experiments are carried out in a tube made of SS-304 with an 11.7 mm diameter and a 1500 mm length to achieve subatmospheric system pressure.

The available literature suggests that flow boiling causes higher pressure fluctuations, affecting flow and wall temperature. Nevertheless, there is limited research on wall temperature distribution in mini-channels. Thus, this study involves experimentally measuring wall temperature distribution and heat transfer coefficient during flow boiling in circular tubes of dimensions 2×300 mm and 4×600 mm. The thermal image technology is employed to visualize the

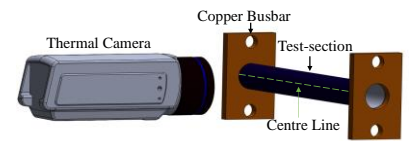
wall temperature distribution and gain valuable insights. This research paper aims to enhance understanding of subcooled boiling at subatmospheric system pressures and shed light on wall temperature distribution during flow boiling in mini-channels. The findings from our experiments can provide valuable information for various applications involving subcooled boiling under similar conditions.

2. Experimental Setup

The experimental setup for atmospheric system pressure consists of a water tank, gear pump, flowmeter, test-sections, thermal camera, DC power unit, vacuum pump, condenser and sump tank, as shown in Fig. 1(A). The test-sections are made of SS-304 material. Three tubes of 2, 4, and 11.7-mm inner diameter and 0.5 mm wall thickness are used as test-section having 300, 600 and 1500-mm lengths, respectively. The thermal camera is painted with black paint of a constant emissivity of 0.92. The copper busbars are soldered at the ends of the test-section to supply constant heat flux. DC power unit supplies the heat input to the test sections. The RTDs are attached to the water tank and sump tank to get the temperatures. The inlet and outlet temperatures are measured by RTDs just before and after the test-sections.



1. Water tank, 2. Gear pump, 3. Flowmeter, 4. Test-section, 5. Thermal camera, 6. DC Power unit, 7. Condenser, 8. Vacuum Pump, 9. Sump tank, T- Temperature (RTD), P- Pressure
(A) Schematic of the atmospheric system experimental setup



(B) Orientation of thermal camera

Fig. 1: Experimental Setup

The test-section is kept in horizontal orientation, as shown in Fig. 1(B). The thermal camera captures images of half tube from one side. The Thermal camera is calibrated for the curved surface. It is assumed that the other half side is symmetrical for horizontal orientation. The one-side half thermal pictures are used to represent the surface temperature in this study. The centre line temperature along the axial direction of the tube, shown in Fig. 1(B), is used to get the heat transfer coefficient. The vacuum pressure pump is utilized to maintain the necessary subatmospheric system pressures. For the subatmospheric system pressure experiments, a test-section having an inner diameter of 11.7mm is utilized.

The gear pump streams the water at a subcooled temperature from the water tank at the specific flow rate. The mass flowmeter measures the flow rate. The test-section is powered by a DC power unit at the required heat flux. The system is kept identical for almost 10 minutes to reach the steady-state. The five thermal images are captured for a single experiment. The readings of the pressure, flowmeter, temperature, current and voltage are saved in the computer using a data logger.

3 Data Reduction

The heat flux (q'') is measured by dividing the heat input (Q) by the outer surface area of the circular tube. The heat input is measured by multiplying the supplied current (I) and voltage (V). The heat transfer coefficient (h) is calculated using the eq (1). The inlet and exit vapor quality (x) at $z=0$ and $z=L$, respectively, are calculated using eq (2).

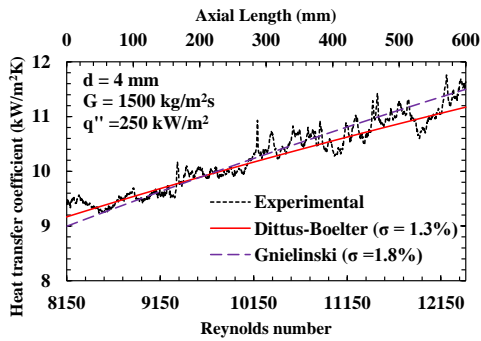
$$\beta = \frac{q''}{T_{wall} - T_{fluid}} \quad (1)$$

$$x = \frac{\frac{Q}{\dot{m}L} - C_p(T_{sat} - T_{in})}{H_{fg}} \quad (2)$$

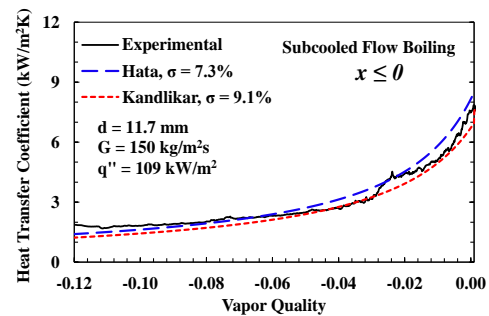
4 Results and Discussion

4.1 Validation of experimental setup

The experiments are performed in liquid phase flow to validate the experimental setup. The heat transfer coefficient in a 4 mm tube is matched with Dittus-Boelter and Gnielinski correlations. The experimental heat transfer coefficient in single-phase flow agrees with the correlations shown in Fig. 2(A). The experimental heat transfer coefficient in 4 mm tube at a mass flux of 1500 kg/m²s and 250 kW/m² heat flux matches with Dittus-Boelter having 1.3% average deviation and with Gnielinski having 1.8% average deviation.



(A) Single-phase flow, $d = 4$ mm



(B) $d = 11.7$ mm, Subcooled flow boiling

Fig. 2: Validation of experimental setups

Fig. 2(B) presents a comparison of the subcooled flow boiling heat transfer coefficient with the correlations developed by the Hata [14] and the Kandlikar [15]. The heat transfer coefficient during subcooled flow boiling exhibits agreement with the available correlations at atmospheric system pressure. Kandlikar's correlation shows an average deviation of 9.1%, while Hata's correlation exhibits an average deviation of 7.3%. The experimental data's trend lines demonstrate similar characteristics to the empirical correlations, as observed from figure 2.

4.2 Temperature contour during single-phase flow in 4 mm tube

In Fig. 3, the graph provides a visual representation of the wall temperature variation during liquid-phase flow in a 4mm channel. An interesting observation is the significant increase in wall temperature along the axial direction, while the wall temperature remains constant in the radial direction. This behavior is a characteristic feature of single-phase flow in conventional channels, where the wall temperature maintains stability and consistency over time. In contrast to flow boiling, where temperature fluctuations occur due to the intermittent formation and collapse of vapor bubbles, single-phase flow does not exhibit such variations. The absence of vapor bubble presence in single-phase flow leads to a smooth and uninterrupted heat transfer process, resulting in a steady wall temperature profile throughout the channel.

The stable wall temperature in single-phase flow allows for predictable and controlled thermal performance, facilitating efficient design and operation of systems. In contrast, flow boiling, with its temperature fluctuations, poses challenges in heat transfer and fluid flow in boiling channels. Insights from Fig. 3 enhance our understanding of fluid dynamics and thermal behavior, leading to improved engineering practices and system optimization.

$$G = 1200 \text{ kg/m}^2\text{s}$$

$$G = 1500 \text{ kg/m}^2\text{s}$$

$$\text{Temp bar } (^\circ\text{C})$$

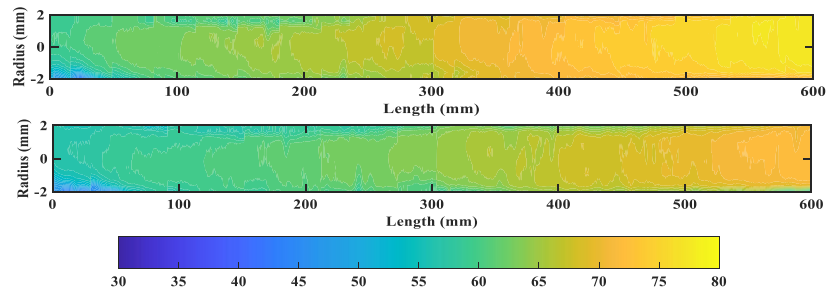


Fig. 3: Temperature distribution in 4 mm tube at $q'' = 200 \text{ kW/m}^2$

4.3 Temperature contour during two-phase flow in 4 mm tube

In a 4 mm tube, the wall temperature distribution is uniform circumferentially in the single-phase, subcooled, and saturated regions. However, the temperature difference between the wall and the fluid varies in these regions. In the single-phase region, this temperature difference is relatively high. As the flow enters the subcooled region, the temperature difference decreases. In the saturated region, the temperature difference is relatively small due to higher boiling heat transfer coefficient. The heat transfer coefficient in the subcooled region increases significantly, which causes a rapid decrease in the wall temperature and leads to fluctuation above the saturation temperature. This, in turn, significantly reduces the circumferential wall temperature difference.

$$G = 600 \text{ kg/m}^2\text{s}$$

$$q'' = 780 \text{ kW/m}^2$$

$$G = 1200 \text{ kg/m}^2\text{s}$$

$$q'' = 780 \text{ kW/m}^2$$

$$\text{Temp bar } (^\circ\text{C})$$

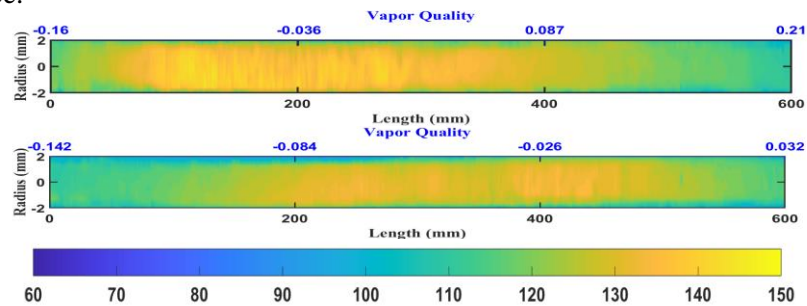


Fig. 4: Wall temperature variation in 4 mm tube during flow boiling

4.4 Temperature contour during two-phase flow in 2 mm tube

In a mini channel, the wall temperature experiences significant fluctuations due to vapor generation within the tube. These oscillations arise due to a decline in heat transfer on the intermittently dried wall, eventually leading to tube damage due to excessive augmentation in wall temperature. The temporal variation of wall temperature at a mass flux of $600 \text{ kg/m}^2\text{s}$ and 400 kW/m^2 heat flux is shown in Fig. 5. Increased heat flux results in a higher generation of vapor bubbles, leading to significant temperature fluctuations with increased frequencies. These fluctuations occur because of reduced heat transfer on the intermittently dried wall, which can ultimately cause damage to the tube due to excessive rise in wall temperature. As a result, studying the flow boiling phenomenon in mini-channels becomes of paramount importance.

$$t = 0.51 \text{ s}$$

$$t = 0.86 \text{ s}$$

$$\text{Temp bar } (^\circ\text{C})$$

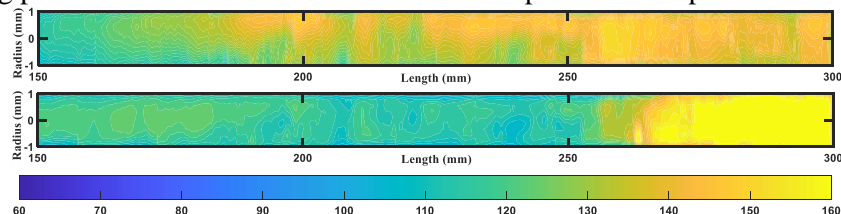


Fig. 5: Wall temperature variation of mini channel at different time

An IR camera is used to observe temperature fluctuations in a mini-channel at different boiling numbers. The fluctuations are recorded for 60 seconds at the middle point ($z = 150$ mm) and endpoint ($z = 300$ mm) of a 2 mm tube. boiling number is gradually increased by raising the heat input while keeping the mass flux constant. Fig. 6(A) that at $Bo = 1.25 \times 10^{-4}$, the wall temperature fluctuates minimally ($\pm 0.8^\circ\text{C}$) with a maximum temperature of 79°C at $z = 300$ mm, staying below the saturation temperature. However, at $Bo = 1.76 \times 10^{-4}$, temperature fluctuations occur due to nucleation initiation. The endpoint of the tube has an average temperature of 99.6°C at this boiling number, leading to bubble generation, flow disturbance, and temperature fluctuations throughout the tube. The mid-point wall temperature ($z = 150$ mm) briefly reaches the saturation temperature due to flow fluctuations caused by vapor bubble generation towards the end of the tube. The duration of higher temperature at the middle point lasts approximately 0.6s due to the rapid exit of vapor bubbles generated towards the tube's end.

At $Bo = 2.24 \times 10^{-4}$, wall temperature fluctuations intensify due to higher nucleation caused by increased heat flux. The average wall temperature at $z = 150$ mm is 91.2°C , and at the endpoint is 99.2°C . At a mass flux of $600 \text{ kg/m}^2\text{s}$, the cycle of temperature fluctuation repeats every 2s at $Bo = 2.24 \times 10^{-4}$. The heat transfer coefficient is calculated in the subcooled region up to $Bo = 2.24 \times 10^{-4}$ by averaging the wall temperature. However, as the heat flux continues to increase, there is a risk of dryout in the 2 mm mini-channel.

In Fig. 6(B), at a mass flux of $1200 \text{ kg/m}^2\text{s}$, the wall temperature remains stable for single-phase flow at $Bo = 9.5 \times 10^{-5}$. By increasing the heat flux to achieve $Bo = 1.38 \times 10^{-4}$, the average wall temperature at the endpoint reaches 96.2°C . Vapor bubble generation at the tube's end affects the midpoint temperature for only 0.2s. With a further increment in heat flux to $Bo = 1.96 \times 10^{-4}$, wall temperature fluctuations intensify at $1200 \text{ kg/m}^2\text{s}$ mass flux, repeating in a cycle every 2.7s. The maximum instantaneous temperature attained at $Bo = 1.96 \times 10^{-4}$ is 167°C . As the Boiling number rises, temperature fluctuations in the subcooled region increase.

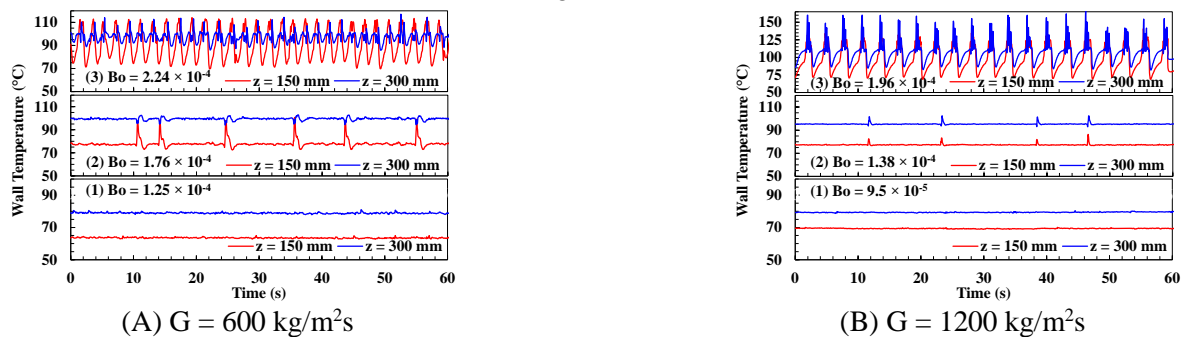


Fig. 6: Wall temperature variation of mini channel at different time

Observations from Fig. 6 reveal that temperature fluctuations are more pronounced at higher boiling numbers during flow boiling. Increasing the heat flux while keeping the mass flux constant results in an escalation of the fluctuations' magnitude. Conversely, at a constant heat flux, temperature fluctuations diminish with higher mass flux values. It's worth noting that the application of the 2 mm diameter mini-channel with highly subcooled water is limited to subcooled flow boiling ($x_{out} < 0$).

4.5 Investigation of subatmospheric system pressure effects on subcooled boiling

The experiments were conducted to gather data on the impact of subatmospheric system pressure on subcooled flow boiling. The experiments are carried out at different mass flux values of 90, and $125 \text{ kg/m}^2\text{s}$. To compare the subcooled boiling heat transfer coefficient under similar boundary conditions, the subatmospheric system pressure was varied at the outlet of the tube, namely 50, and 75kPa, using a vacuum pump. The heat flux was gradually varied within the range of $73 - 109 \text{ kW/m}^2$. Fig. 7 presents the comparison of subcooled flow boiling heat transfer coefficient at the different mass flux and heat flux conditions: $G = 90 \text{ kg/m}^2\text{s}$, $q'' = 73 \text{ kW/m}^2$ in Fig. 7(A), and $G = 125 \text{ kg/m}^2\text{s}$, $q'' = 109 \text{ kW/m}^2$ in Fig. 7(B).

The surface temperature of the test tube determines the flow regime, either single-phase or subcooled boiling. Initially, heat transfer occurs through forced convection from the inner surface to the water, leading to a gradual increase in heat

transfer coefficient in the axial direction. The heat transfer coefficient rises with increasing liquid Reynolds number at a constant mass flux and higher bulk fluid temperature. When the internal surface temperature surpasses the working fluid's saturation temperature at the system pressure, nucleation starts, and subcooled flow boiling occurs until the vapor quality approaches zero [17]. At onset of nucleate boiling, the wall temperature changes its slope. Bubble formation and growth take place at discrete sites during nucleation, resulting in an abrupt increase in the subcooled boiling heat transfer coefficient along the axial direction. Subcooled flow boiling involves simultaneous occurrences of single-phase convection and nucleation boiling.

Fig. 7 indicates that the subcooled flow boiling heat transfer coefficient is higher at lower system pressure under the same boundary conditions. The increased number of bubble nucleation sites at higher surface temperatures leads to a sharp heat transfer coefficient increase up to zero vapor quality at all system pressures. Subatmospheric system pressure alters the transport and thermophysical characteristics of liquid and vapor phases, resulting in larger vapor bubbles at lower subatmospheric system pressure. These larger bubbles carry more heat away from the surface, enhancing the subcooled boiling heat transfer coefficient due to the stronger buoyancy force aiding in bubble detachment.

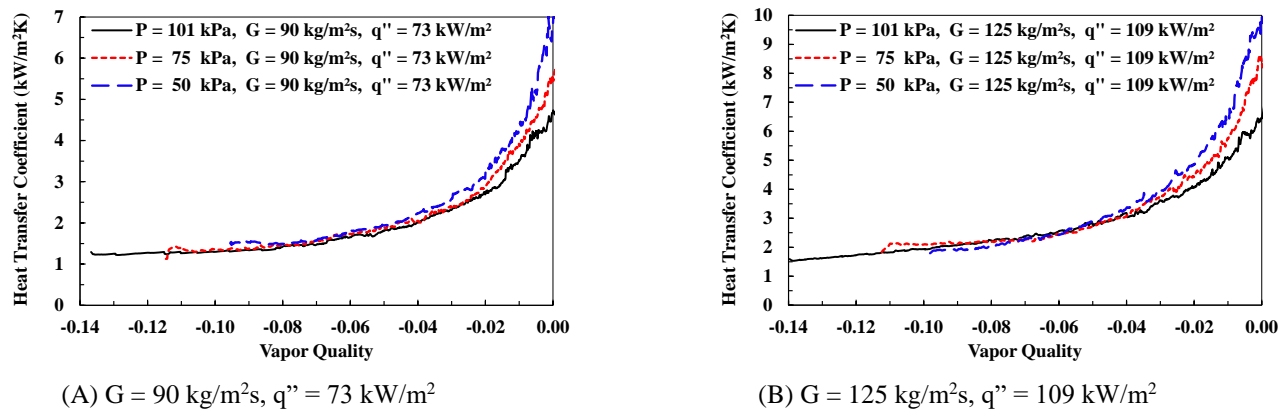


Fig. 7. Subatmospheric system pressures effect on subcooled boiling heat transfer coefficient

5. Conclusion

The flow boiling is investigated in two tubes of 2 and 4 mm diameters with 300 and 600 mm length at atmospheric pressure. Boiling heat transfer coefficient and wall temperature distribution are analysed in small diameter tubes. Subcooled flow boiling at subatmospheric system pressures of 50 and 75 kPa is investigated in 11.7 mm tube.

The heat transfer coefficient in 4 mm tube agrees with Dittus-Boelter and Gnielinski's correlation in liquid-phase flow. Kandlikar's correlation is compared in the two-phase flow. The wall temperature is not varied radially significantly during liquid-phase flow. The wall temperature is varied during two-phase flow significantly in mini-channels.

The subcooled flow boiling heat transfer coefficient is notably influenced by subatmospheric system pressure. In all examined states, the subcooled flow boiling heat transfer coefficient is higher at lower system pressure compared to atmospheric pressure. Mass flux does not have a major effect on the subcooled flow boiling heat transfer coefficient at subatmospheric system pressure.

The wall temperature in the mini channel exhibited fluctuations over time, primarily caused by the boiling process. However, up to a boiling number of 1.76×10^{-4} , the amplitude of these fluctuations was notably lower, resulting in a more stable and consistent heat transfer process over time.

Moreover, the subcooled flow segment's heat transfer coefficient at subatmospheric system pressures increases with higher heat flux, leading to the commencement of more nucleation sites. The axial length for subcooled boiling is larger at lower heat flux and lower mass flux. Overall, the heat transfer coefficient is higher in subcooled flow boiling under higher mass flux, higher heat flux, and lower system pressure conditions.

References

- [1] A. Kumar and B. K. Hardik, "Heat transfer distribution and pressure fluctuations during flow boiling in a pipe with different orientations," *Appl. Therm. Eng.*, vol. 201, p. 117822, Jan. 2022.
- [2] S. G. Kandlikar, M. E. Steinke, S. Tian, and L. A. Campbell, "High-speed photographic observation of flow boiling of water in parallel mini-channels," *Proc. 35th Nat. Heat Transf. Conf.*, Anaheim, California, pp. 1–10, 2001.
- [3] K. E. Kasza, T. Didascalou, and M. W. Wambsganss, "Microscale flow visualization of nucleate boiling in small channels: Mechanisms influencing heat transfer," in *proceedings of the international conference on Compact Heat Exchangers for the Process Industries*, Begell House Inc., New York, 1997, pp. 343–352.
- [4] W. Yu, D. M. France, M. W. Wambsganss, and J. R. Hull, "Two-phase pressure drop, boiling heat transfer, and critical heat flux to water in a small-diameter horizontal tube," *Int. J. Multiph. Flow*, vol. 28, no. 6, pp. 927–941, Jun. 2002.
- [5] J. Kim and J. S. Lee, "Numerical study on the effects of inertia and wettability on subcooled flow boiling in microchannels," *Appl. Therm. Eng.*, vol. 152, pp. 175–183, Apr. 2019.
- [6] J. Wang, K. Lu, S. Lu, and H. Zhang, "Experimental study on ceiling temperature profile of sidewall fires at reduced pressure in an aircraft cargo compartment," *Exp. Therm. Fluid Sci.*, vol. 82, pp. 326–332, Apr. 2017.
- [7] N. Colgan, J. L. Bottini, Z. J. Ooi, and C. S. Brooks, "Experimental study of wall nucleation characteristics in flow boiling under subatmospheric pressures in a vertical square channel," *Int. J. Heat Mass Transf.*, vol. 134, pp. 58–68, 2019.
- [8] Z. Rahimi-Ahar, M. S. Hatamipour, Y. Ghalavand, and A. Palizvan, "Comprehensive study on vacuum humidification-dehumidification (VHDH) desalination," *Appl. Therm. Eng.*, vol. 169, p. 114944, Mar. 2020.
- [9] Z. Xiong, C. Ye, M. Wang, and H. Gu, "Experimental study on the sub-atmospheric loop heat pipe passive cooling system for spent fuel pool," *Prog. Nucl. Energy*, vol. 79, pp. 40–47, Mar. 2015.
- [10] S. Singh, P. R. Chakraborty, and H. B. Kothadia, "Experimental study on energy transformation of static liquid pool during flash evaporation," *Appl. Therm. Eng.*, vol. 220, p. 119712, Feb. 2023.
- [11] N. Colgan, J. L. Bottini, R. Martínez-Cuenca, and C. S. Brooks, "Experimental study of critical heat flux in flow boiling under subatmospheric pressure in a vertical square channel," *Int. J. Heat Mass Transf.*, vol. 130, pp. 514–522, Mar. 2019.
- [12] K. Latsch, F. Morell, and H. Rampf, "Subcooled forced convection boiling heat transfer at subatmospheric pressure," *PROC. 6TH INT. HEAT TRANSF. CONF. (TORONTO, CANADA AUG. 7-11, 1978)*, Washingt. D.C., U.S.A., Hemisph. CORP., 1978, vol. 1, pp. 287–292.
- [13] W. R. Chang, C. A. Chen, J. H. Ke, and T. F. Lin, "Subcooled flow boiling heat transfer and associated bubble characteristics of FC-72 on a heated micro-pin-finned silicon chip," *Int. J. Heat Mass Transf.*, vol. 53, no. 23–24, pp. 5605–5621, Nov. 2010.
- [14] K. Hata and S. Masuzaki, "Critical heat fluxes of subcooled water flow boiling in a short vertical tube at high liquid Reynolds number," *Nucl. Eng. Des.*, vol. 240, no. 10, pp. 3145–3157, Oct. 2010.
- [15] S. G. Kandlikar, "Development of a flow boiling map for subcooled and saturated flow boiling of different fluids inside circular tubes," *J. Heat Transfer*, vol. 113, no. 1, pp. 190–200, Feb. 1991.
- [16] W. Gao, J. Qi, X. Yang, J. Zhang, and D. Wu, "Experimental investigation on bubble departure diameter in pool boiling under sub-atmospheric pressure," *Int. J. Heat Mass Transf.*, vol. 134, pp. 933–947, May 2019.
- [17] A. Kumar and H. Kothadia, "Experimental Analysis of Subcooled Flow Boiling at Subatmospheric Pressure," *Proc. 26th National 4th Int. ISHMT-ASTFE Heat Mass Transf. Conf. December 17-20, 2021, IIT Madras, Chennai-600036, Tamil Nadu, India*, pp. 1779–1784, Feb. 2021.